Genome-wide RNA interference screen identifies previously undescribed regulators of polyglutamine aggregation

Ellen A. A. Nollen*†, Susana M. Garcia†‡, Gijs van Haaften*, Soojin Kim‡, Alejandro Chavez‡, Richard I. Morimoto†‡§, and Ronald H. A. Plasterk*†§

*Division of Functional Genomics, Hubrecht Laboratories/Netherlands Institute for Developmental Biology, 3584 CT Utrecht, The Netherlands; and ‡Department of Biochemistry, Molecular Biology, and Cell Biology, Rice Institute for Biomedical Research, Northwestern University, Evanston, IL 60208

Edited by A. L. Horwich, Yale University School of Medicine, New Haven, CT, and approved February 13, 2004 (received for review November 19, 2003)

Protein misfolding and the formation of aggregates are increasingly recognized components of the pathology of human genetic disease and hallmarks of many neurodegenerative disorders. As exemplified by polyglutamine diseases, the propensity for protein misfolding is associated with the length of polyglutamine expansions and age-dependent changes in protein-folding homeostasis, suggesting a critical role for a protein homeostatic buffer. To identify the complement of protein factors that protects cells against the formation of protein aggregates, we tested transgenic *Caenorhabditis elegans* strains expressing polyglutamine expansion yellow fluorescent protein fusion proteins at the threshold length associated with the age-dependent appearance of protein aggregation. We used genome-wide RNA interference to identify genes that, when suppressed, resulted in the premature appearance of protein aggregates. Our screen identified 186 genes corresponding to five principal classes of polyglutamine regulators: genes involved in RNA metabolism, protein synthesis, protein folding, and protein degradation; and those involved in protein trafficking. We propose that each of these classes represents a molecular machine collectively comprising the protein homeostatic buffer that responds to the expression of damaged proteins to prevent their misfolding and aggregation.

protein misfolding | neurodegenerative diseases

Accumulation of misfolded proteins in protein aggregates is a hallmark of various aging-associated diseases, including Alzheimer's and Parkinson's diseases, amyotrophic lateral sclerosis, and polyglutamine expansion disorders, which includes Huntington's disease and spinocerebellar ataxias (1–4). The biochemical properties of the affected proteins dictate not only their propensity to aggregate but also the age of onset of these diseases. This is particularly apparent for polyglutamine expansion disorders in which the aggregation properties of polyglutamine proteins and the age of onset of disease directly correlate with the length of the polyglutamine stretch in the disease protein (5–7).

These features of length and age dependence of polyglutamine aggregation have been reconstituted in transgenic *Caenorhabditis elegans* strains expressing polyglutamine expansions as yellow fluorescent protein (YFP) fusion proteins (8, 9). Whereas animals expressing YFP fusions with polyglutamine stretches up to 24 residues (Q24) show diffuse YFP staining in all muscle cells throughout their life, animals with a Q stretch length of 40 residues or longer show an early-onset punctate localization corresponding to immobile protein aggregates. Unlike animals expressing Q24 or Q40, however, those expressing the threshold length, Q33 and Q35, displayed an intermediate phenotype in both age of onset and number of aggregates. All Q lengths show variability in aggregation from cell to cell within individual animals. The aggregation behavior can be influenced by the genetic background of the animal. For example, aggregation of Q40 and Q82 YFP is greatly delayed in the aging mutant *age-1* (9). Conversely, knock-down of heat-shock protein (Hsp)16, a downstream target of the insulin signaling pathway with elevated expression in the *age-1* mutant, results in enhancement of aggregate formation of Q40 YFP (10). The observation that the threshold of aggregation can be genetically influenced reveals the potentially important role of different pathways in the formation of polyglutamine aggregates.

Materials and Methods

Strains. Construction of the Q0, Q24, Q33, Q35, and Q40 strains, expressing YFP fused to stretches of 0, 24, 33, 35, and 40 glutamine residues, has been described (9). Transgenes were integrated by exposing the animals to γ-ray irradiation. Animals were outcrossed five times.

Fluorescence Microscopy and Fluorescence Recovery After Photobleaching (FRAP). Animals were mounted on a 2% agar pad on a glass slide and immobilized in 0.01 M azide. Fluorescence micrographs were taken by using a Zeiss Axioplan 2/LSM 510 META confocal microscope. Immobilized animals were subjected to FRAP analysis as described (11) with the following modifications. Images were taken with ×63/1.4 oil differential interference contrast objective at seventh zoom power with the 514-nm line for excitation. An area of 3.6 μm^2 was bleached for 4 s (five iterations at 100% laser power), after which an image was collected every 30 s (at 0.1% laser power). Relative fluorescence intensity (RFI) was determined by using RFI = $(Ne_t/N1_t)/(Ne_0/N1_0)$ equation. Ne_t is the average intensity of the bleached area at a given time point, and $N1_t$ is the average intensity of an adjacent nonbleached area at the corresponding time points as a control for general photobleaching and background fluorescence. Ne_0 and $N1_0$ are the average intensity before photobleaching of the bleached or nonbleached control area, respectively.

Immunoblotting Analysis. Extracts were prepared by sonication of animals that were resuspended in PBS. Laemmli sample buffer was added to the lysates to a final concentration of 1% SDS. Samples were boiled for 5 min and analyzed by 12.5% SDS/PAGE and Western blot analysis. Blots were probed with a 1:5,000 dilution of anti-GFP peptide polyclonal antiserum (12). Antibody binding was visualized by binding of horse-

BIOCHEMISTRY

This paper was submitted directly (Track II) to the PNAS office.

Abbreviations: RNAi, RNA interference; YFP, yellow fluorescent protein; Q stretch, polyglutamine stretch; Q*n*, Q stretch of *n* residues; FRAP, fluorescence recovery after photobleaching; dsRNA, double-stranded RNA.

†E.A.A.N., S.M.G., R.I.M., and R.H.A.P. contributed equally to this work.

§To whom correspondence may be addressed. E-mail: r-morimoto@northwestern.edu or plasterk@niob.knaw.nl.

radish peroxidase-coupled secondary antibody and chemiluminescence (ECL Western blotting detection reagents, Amersham Pharmacia).

Screen. The full-genome RNAi screen was performed in a 96-well format by feeding RNAi bacteria to animals in liquid culture. Animals were synchronized by NaOCl bleaching and overnight hatching in M9. In each well, 10–15 L1 larval stage animals were suspended in 50 μl of M9 plus [M9, 10 μg/ml cholesterol, 50 μg/ml ampicillin, 12 μg/ml tetracycline, 200 μg/ml isopropyl β-D-thiogalactoside (IPTG) and 0.1 μg/ml fungizone] and added to 80 μl of an overnight culture of RNAi bacteria induced by IPTG for 4 h. The animals were grown at 23°C with continuous shaking at 150 rpm (New Brunswick Scientific Incubation shaker). The animals were scored for foci formation by visual inspection after 72 h. RNAi-producing bacteria that induced more than five visible foci in >30% of the animals in a well were scored as aggregation enhancers. All positive RNAi foods were confirmed in an independent experiment and scored for aggregate formation in Q0, Q24, and Q33 animals. The gene targets of the positive RNAi foods were verified by sequencing of the insert of the RNAi plasmids.

Results

To identify genes that prevent protein aggregate formation, we used a *C. elegans* strain expressing Q35 YFP. Q35 animals exhibit a diffuse YFP staining pattern in all expressing cells from the moment they hatch through young adulthood. From young adulthood onward, aggregates become gradually visible in a subset of the muscle cells (9). The age of aggregate onset is invariable and occurs after the animals reach adulthood at the fifth day after hatching.

To determine whether aggregation of Q35 YFP can be enhanced genetically, we tested whether known modifiers of polyglutamine protein toxicity can induce the premature appearance of aggregates in Q35 YFP animals upon selective knock-down by RNAi. In mammalian cells and *Drosophila* models of Huntington's disease or spinocerebellar ataxia 1, suppressors of polyglutamine toxicity were identified such as the molecular chaperone Hsp70, a subset of its J domain- or tetratricopeptide repeat domain-containing cochaperones and the heat shock transcription factor, heat-shock factor (HSF)-1 (13–16). We searched the *C. elegans* genome for all Hsp70-, J domain-, and TPR domain-containing genes as well as HSF-1 by using similarity and domain searches (Table 2, which is published as supporting information on the PNAS web site). *Escherichia coli* strains expressing double-stranded RNA for each of these genes were fed to synchronized L1 larvae of Q0, Q24, Q33, Q35, and Q40 animals. We used L1 larvae to avoid the predicted embryonic lethality of many of these genes. The animals were examined for YFP foci formation after 3 days on RNAi food, corresponding to 1 day before the normal onset of polyglutamine aggregation.

Of the 72 candidate genes, the knock-down of only four resulted in the appearance of foci in Q33 and Q35 animals that were similar to the foci observed in Q40 animals. These include two Hsp70 genes (F26D10.3 and C37H5.8), a single J domain gene (F18C12.2), and *hsf-1* (Y53C10.A12) (Fig. 1 *H*, *I*, *M*, and *N*, and Table 2). An important validation of our screen was that no foci were observed when the same genes were knocked down in either Q0 or Q24 animals (Fig. 1 *F*, *G*, *K*, and *L*), revealing specificity of this assay for polyglutamine-expansion-dependent aggregation. We assessed whether the fluorescent foci that appeared in RNAi-treated Q35 animals were biophysically and biochemically similar to polyglutamine aggregates of animals expressing longer Q stretches. Polyglutamine proteins that associate to form aggregates exhibit reduced *in vivo* mobility as monitored by using FRAP (11). Photobleaching of diffused Q0 YFP or Q35 YFP led to an immediate recovery of the fluorescence to 100% of the initial level (Fig. 1 *P*, *R*, and *U*), consistent with the biophysical properties of soluble proteins. In contrast, only 30% of the fluorescent signal associated with foci in Q35 animals, in which *hsp-1* or *hsf-1* was knocked down by RNAi, recovered after photobleaching consistent with the biophysical properties of an immobilized state (Fig. 1 *S*, *T*, and *U*). Moreover, the lack of fluorescence recovery for the Q35 aggregates was kinetically and quantitatively similar to that observed for Q40 aggregates (Fig. 1 *Q* and *U*). These results demonstrate that Q35 YFP converts from a soluble to an aggregated state when the levels of *hsp-1* or *hsf-1* are reduced.

Another biochemical characteristic of polyglutamine aggregates is their resistance to the detergent SDS (6, 17), and this was assessed by SDS/PAGE followed by Western blot analysis using an antibody against YFP. Q0 YFP and Q24 YFP, in *hsp-1* and *hsf-1* knock-down animals, exhibited a mobility according to their calculated molecular masses of 29 and 32 kDa, respectively (Fig. 1*V*, lanes 1 and 5–7). In extracts from Q40 animals, however, Q40 YFP was detected as two species corresponding to the predicted size of Q40 YFP and a higher molecular mass species retained at the top of the gel (Fig. 1*V*, lane 8), likely corresponding to SDS-insoluble aggregates. Q35 YFP from lysates of animals in which *hsp-1* or *hsf-1* were knocked down showed increased levels of the high molecular mass band compared to Q35 animals fed with bacteria containing an empty vector (Fig. 1*V*, lanes 2–4). These results demonstrate that the Q35 YFP foci, induced by RNAi for *hsp-1* and *hsf-1*, exhibit biochemical properties indistinguishable from polyglutamine aggregates formed from proteins with longer stretches of polyglutamine.

Having established the utility of the Q35 YFP animals to identify suppressors of polyglutamine aggregation, we performed a genome-wide RNAi feeding library screen. The RNAi library contains *E. coli* strains expressing double-stranded RNAs for 16,757 of the 19,427 predicted individual *C. elegans* genes (18). L1 larvae were transferred to the different RNAi foods. After 3 days, the animals were examined for the presence of fluorescent foci. Of the 16,757 genes tested, after rescreening in triplicate, 186 genes consistently induced an earlier onset of aggregation phenotype in Q35 animals. This collection of positives was subsequently counterscreened with Q0 and Q24 YFP-expressing animals to remove any genes that were unrelated to the polyQ length-dependent aggregation phenotype. We also tested Q33 YFP animals to confirm independently the effects of these genes on the aggregation phenotype. All 186 genes induced an early onset of foci formation in both Q33- and Q35-expressing animals and not in Q0 and Q24 animals, indicating that the identified genes have a role in the prevention of polyglutamine aggregation. The list of genetic modifiers of aggregation can be categorized into five major classes: genes involved in RNA metabolism, protein synthesis, protein folding, protein trafficking, and components of the proteasome (Table 1, Table 3, which is published as supporting information on the PNAS web site, and Fig. 2 *A*–*C*).

To assess whether the identified modifiers affected the biochemical state of polyglutamine proteins, we examined whether the knock-down of 16 randomly selected genes of the 186 positives influenced the solubility of Q35 YFP analyzed by SDS/PAGE and Western blotting (Fig. 2*D*). An increase in the fraction of insoluble Q35 YFP comparable to the increase induced by RNAi for *hsp-1* and *hsf-1* was observed (Fig. 2*D*, lanes 4–8, 11–14, 18–22, 26–30, 33–36, and 40–44). The effect was Q length-dependent, because no change in Q24 YFP solubility was observed (Fig. 2*D*, lanes 1–3, 9–10, 15–17, 23–25, 31–32, and 37–39). Our results suggest that at least 186 genes are involved in suppressing polyglutamine aggregation.

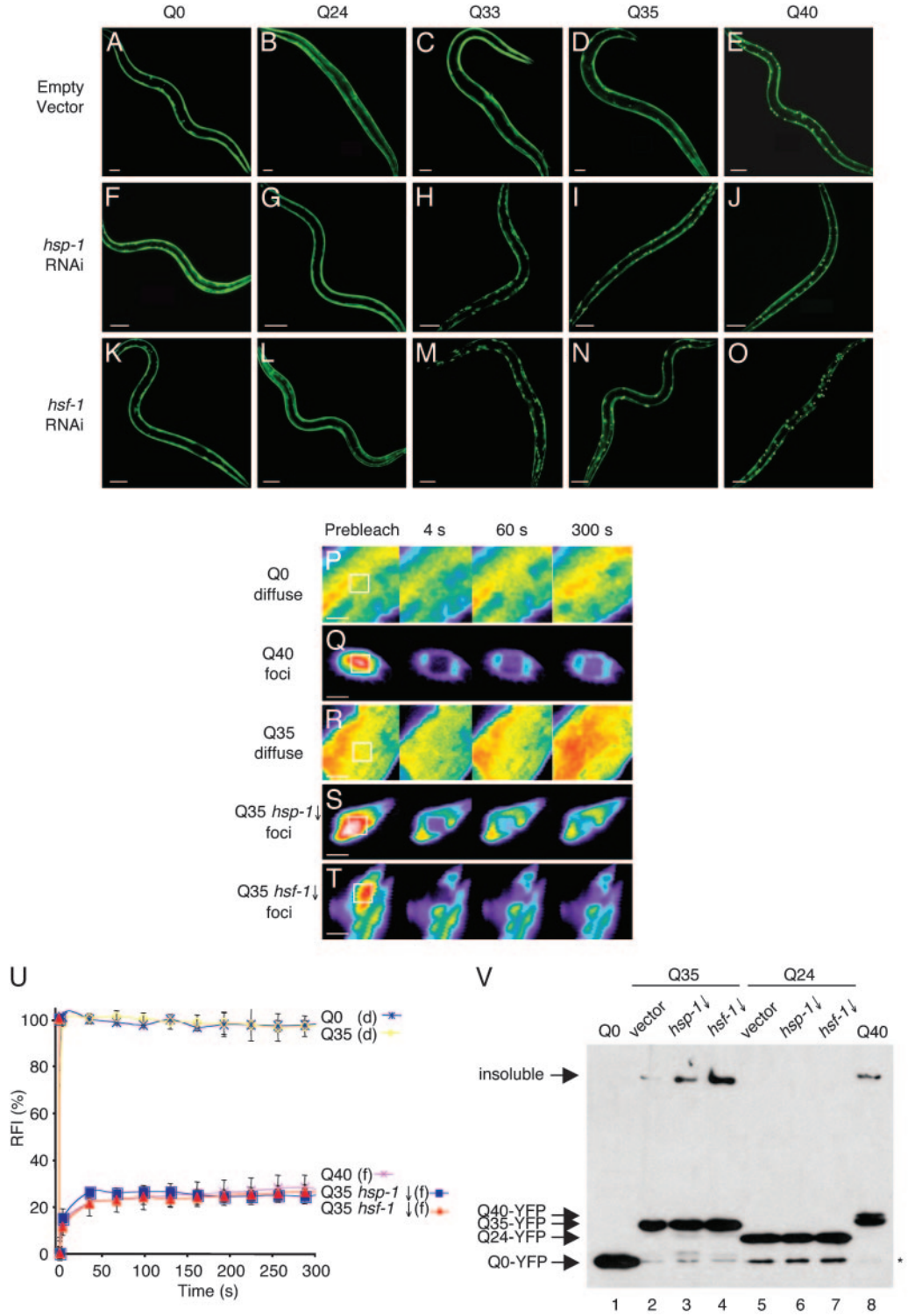

Fig. 1. RNAi for *hsp-1* (F26D10.3) and *hsf-1* (Y53C10.A12) induces aggregate formation of polyglutamine YFP proteins in a Q stretch length-dependent manner. (*A–O*) Fluorescence microscopy pictures of 4-day-old *C. elegans* expressing polyglutamine YFP with Q stretches of 0 (*A*, *F*, and *K*), 24 (*B*, *G*, and *L*), 33 (*C*, *H*, and *M*), 35 (*D*, *I*, and *N*), and 40 residues (*E*, *J*, and *O*). Animals were synchronized to the L1 stage and fed for 72 h with bacteria containing an empty vector (*A–E*), double-stranded RNA (dsRNA) against *hsp-1* (*F–J*), or dsRNA against *hsf-1* (*K–O*). (Bar = 50 μm.). (*P–U*) Aggregates of Q35 YFP induced by RNAi for *hsp-1* or *hsf-1* are biophysically similar to aggregates of Q40-YFP. FRAP analysis of the mobility of diffusely stained (*P* and *R*) or aggregated (*Q*, *S*, and *T*) Q0 YFP (*P*), Q40 YFP (*Q*), or Q35 YFP (*R–T*) fed with control bacteria (*R*), bacteria expressing dsRNA against *hsp-1* (*S*), or bacteria expressing dsRNA against *hsf-1* (*T*). (Bar = 2 μm.) Fluorescent molecules in the boxed area (white box) were subjected to FRAP analysis. Single scanned images were taken before (prebleach) and at the indicated time points after photobleaching. (*U*) Quantitative FRAP analysis of soluble or aggregate-associated YFP fusion proteins. The relative fluorescence intensity was determined for each time point and was represented as the average of the analysis of three independent measurements. Error bars indicate SEM. (*V*) Aggregates of Q35 YFP induced by RNAi for *hsp-1* or *hsf-1* are biochemically similar to aggregates of Q40 YFP. Extracts of animals expressing YFP fusion proteins were separated by SDS/PAGE and immunoblotted with an anti-YFP antibody. Lysates of Q0 animals (lane 1), lysates of Q35 animals or Q24 animals fed with empty vector (lanes 2 and 5), *hsp-1* RNAi food (lane 3 and 6), or *hsf-1* RNAi food (lanes 4 and 7). Asterisk indicates degradation products.

BIOCHEMISTRY

Table 1. Overview of modifiers of polyglutamine aggregation (see Table 3 for full list of genes)

Cellular process (no. of genes)*	Function (no. of genes)*†	Cosmid no.	Gene example	Gene description	Mammalian homologue
RNA synthesis and processing (38)	Synthesis (14)	F36A4.7	*ama-1*	Largest subunit of RNA polymerase II	RPB1
	Splicing (19)	T13H5.4	*phi-9*	Putative U2 snRNP-associate splicing factor	SAP61/SF3a60
Protein synthesis (53)	Initiation (5)	Y39G10AR.8	*eif-2*	Translation initiation factor *eIF2*	eIF-2-γ
	Elongation (4)	F25H5.4	*eft-2*	Elongation factor 2	eEF1A-2
	Ribosomal subunit (40)	F39B2.6	*rps-26*	Ribosomal protein S26	40S ribosomal protein S26
Protein folding (10)	Chaperonin (6)	C07G2.3	*cct-5*	Homologue chaperonin TCP-1, subunit 5 (ε)	TCP-1-ε
	Hsp70 (2)	C37H5.8	*hsp-6*	Member of the heat-shock HSP70 protein family	GRP75
	DnaJ (1)	F18C12.2	*rme-8*	Heat-shock protein DnaJ, N-terminal	Unknown
Protein transport (25)	Vesicle (14)	C39F7.4	*rab-1*	GTP-binding protein of the rab family	RAB-1A
	Nuclear import (5)	C53D5.6	*imb-3*	Putative karyopherin β	Importin β-3 subunit
	Cytoskeleton (6)	C36E8.5	*tbb-2*	Member of the β-tubulin protein family	Tubulin β-2 chain
Protein degradation (14)	19S (4)	F56H1.4	*rpt-5*	Putative ATPase subunit of the 19S regulatory complex	26S protease regulatory subunit 6A
	20S (7)	C36B1.4	*pas-4*	Putative α4 20S proteasome core subunit	Proteasome subunit α type 7
	Ubiquitin like (1)	F52C6.3	*phi-37*	Member of the ubiquitin family	Ubiquitin C
	E1 Ub-activating enzyme (1)	C47E12.5	*uba-1*	Similarity to ubiquitin-activating enzyme E1	Ubiquitin activating enzyme E1
Other (46)	ATP synthesis (6)	H28O16.1	*phi-44*	Putative ATP synthase	ATP synthase α chain mitochondrial precursor

*Number of genes found in the indicated categories.
†Major functional groups from each category of cellular process.

Based on the nature of previously reported suppressors and enhancers of polyglutamine aggregation, we expected that a subset of the genes would play a role in protein quality control and thus prevent accumulation of misfolded proteins (13–16). Such genes would include molecular chaperones and components of the proteasomal degradation machinery (Fig. 3). Indeed, we did identify molecular chaperones and genes involved in proteasomal degradation, although unexpectedly, only a very few predicted chaperones and cochaperones were identified as suppressors; these include two members of the Hsp70 family, a single DnaJ domain protein, and six of the eight subunits of cytosolic chaperonin 1, which is the homologue of the mammalian TCP-1 chaperonin (Tables 1 and 3) (19). Of particular note, down-regulation of neither Hsp90 nor Hsp16 had any consequence on polyglutamine aggregation in our screen. Genes involved in protein degradation included 7 of 14 subunits of the 20S core of the proteasome, 4 putative subunits of the 19S cap (1 of 6 ATPases and 3 of 12 non-ATPases), 1 ubiquitin-like protein, and enzymes involved in ubiquitin activation and deubiquitination (Table 1).

The identification of only two Hsp70s and one DnaJ domain protein suggests specificity among the chaperone genes that is supported independently by the results of screens in *Drosophila* and candidate gene studies demonstrating that Hsp70 and the J domain proteins, like Hdj-1/Hsp40, can suppress aggregation and toxicity (14–16). The role(s) of chaperones and the degradative machinery reveals the importance of proteins that actively suppress aggregation, for example, as a chaperone shielding the unfolded domain of the protein or by regulating the turnover of the polyglutamine protein.

Another class of genes that may play a role in the clearance of misfolded proteins consists of the protein transport genes, such as tubulin, actin, and nuclear import factors (Tables 1 and 3). Transport along microtubules has been suggested as a mechanism to sequester misfolded proteins at the centrosome of cells in so-called "aggresomes," which would prevent inappropriate associations with other cellular components and concentrate these proteins for proteasomal degradation (20). Perhaps the inability of early oligomeric states of the polyglutamine proteins to be properly transported resulted in the premature appearance of aggregates. Moreover, the finding of the CCT-1 complex, which has chaperone activity for actin and tubulin, is consistent with a role for cytoskeletal dynamics in the appearance of polyglutamine aggregates (19). Recent findings show that the CCT complex interacts with nonnative proteins other than actin and tubulin as well, including a number of β-sheet-containing WD repeat proteins (21–23). A broader specificity of CCT-1 for β-sheet-containing substrates could suggest that the CCT complex suppresses aggregation through a direct interaction with the polyglutamine protein.

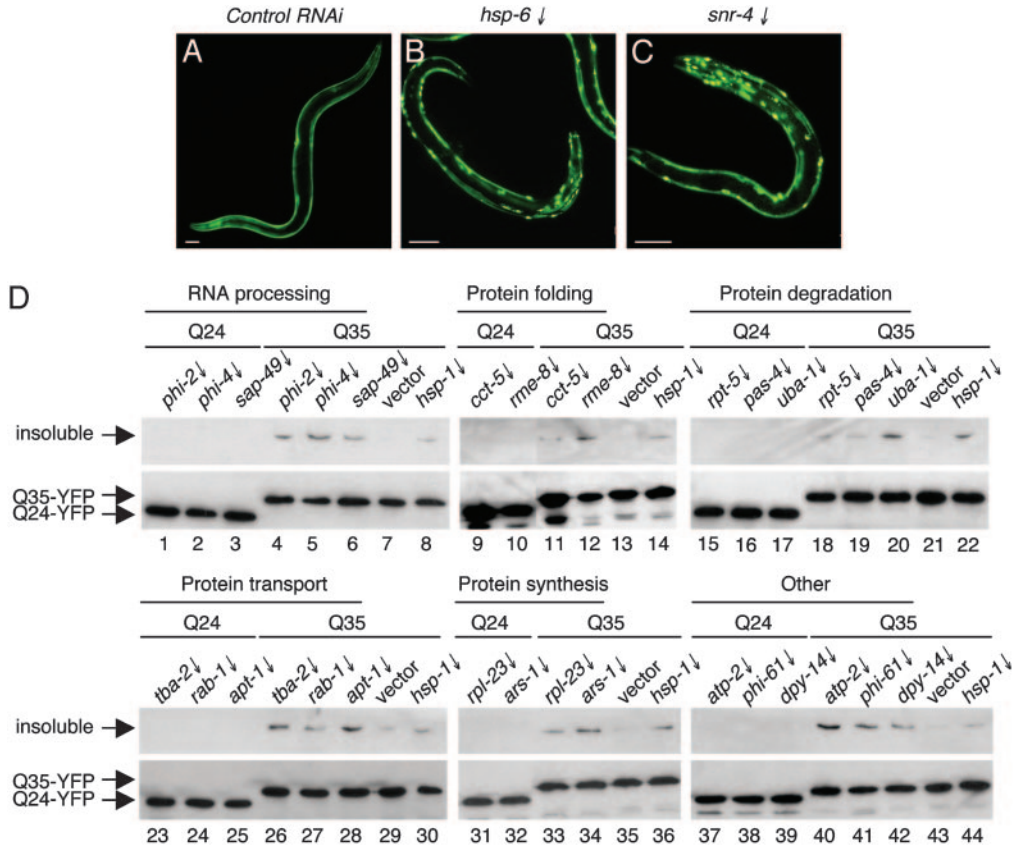

Fig. 2. RNAi for newly identified modifiers of polyglutamine aggregate formation induces aggregates and insolubilization of polyglutamine proteins that depend on the length of the Q stretch. (*A–C*) Fluorescence microscopy pictures of 4-day-old *C. elegans* expressing Q35 YFP fed with control RNAi food (*A*) and two examples of positive clones expressing dsRNA against *hsp-6* (*B*) and *snr-4* (*C*). (Bar = 50 μm.) (*D*) Western blot analysis of extracts of animals expressing Q24 YFP or Q35 YFP, fed with bacteria expressing dsRNA for the indicated genes. Genes are grouped according to their functional classes.

Our results reveal that maintenance of protein homeostasis requires a balance that extends well beyond the immediate involvement of chaperone-mediated folding and proteasomal degradation. In addition to the protein quality control genes, 38 genes involved in RNA synthesis and processing were identified, of which 19 have a role in splicing. Moreover, 53 genes with a role in protein synthesis were identified of which 40 encode components of the large and small subunits of the ribosome (Tables 1 and 3). For these classes of genes, several possible mechanisms can be envisioned for how their knock-down could enhance aggregation: (*i*) by increasing the influx of misfolded proteins, by causing RNA processing defects, or by the synthesis of proteins by an imperfect translational machinery; or (*ii*) by disrupting the equilibrium among synthesis, folding, and degradation. Down-regulation of a ribosomal subunit, for example, could result in the appearance of missense mutations and consequently misfolded proteins or could alter the composition of nascent polypeptides, which then could alter the availability of chaperones. Such deregulation of the translation machinery could be sensed by the degradative machinery and could result in down-regulation of the proteasome, with the consequence that the aggregation-prone polyglutamine protein Q35 undergoes premature aggregation.

Discussion

Our findings reveal that the transition between a soluble or aggregated state of polyglutamine proteins is governed by a much more complex integration of biosynthetic events that regulates the appearance and degradation of proteins beyond the balance of chaperones and the proteasome. The identification of

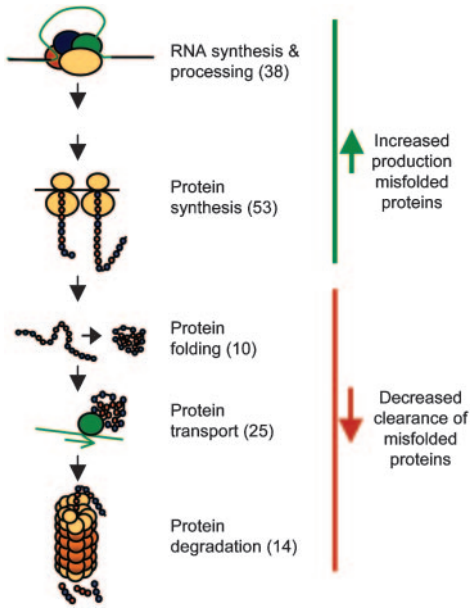

Fig. 3. Overview of modifiers of polyglutamine aggregation. Represented are the five major classes of genes of which knock-down by RNAi enhances polyglutamine aggregate formation. We propose that knock-down of genes in these classes induces aggregate formation either by an increase in the production of misfolded proteins (green line) or by a decrease in the clearance of misfolded proteins (red line). Between brackets is the number of genes found in the indicated functional class.

genes involved in RNA processing and protein synthesis and the major classes of suppressors of protein misfolding leads us to suggest an important role for macromolecular biosynthetic protein machines as "sensors" of protein damage. It is intriguing that down-regulation of individual components alone has dominant effects on protein misfolding, causing an immediate imbalance in protein homeostasis, given an expectation that the buffering capacity for protein-folding quality control must be comprised of many components. This suggests that the composition of the protein-folding proteome is delicately balanced and highly sensitive to changes initiated by the expression of proteins such as those containing polyglutamine expansions.

A recently published genome-wide screen for enhancers of polyglutamine toxicity in yeast supports this notion. In that screen, a mutant fragment of Huntingtin with an expanded polyglutamine stretch exhibited a lethal phenotype when expressed in the background of 52 individual single gene deletion mutants (24). A large fraction of these genes are predicted to have a role in protein folding or degradation, revealing the involvement of a common functional class of genes in both *Saccharomyces cerevisiae* and *C. elegans*. Curiously, no direct yeast orthologs of the 186 enhancers of polyglutamine aggregation that we identified were found. One possible explanation for these differences is that yeast deletion strains for essential genes are not viable. Conversely, a limitation of our RNAi screen is the inherent variability in the level of mRNA knock-down for different genes and tissues (25, 26). Although we have identified 186 genes that exhibit a clear phenotype in our assay, other genes may have been overlooked because the level of knock-down was insufficient. For some genes, we have previously assayed the reduction of gene expression after RNAi; for example, we saw >90% reduction for chaperones (27). We have not tested this for all genes, because the percentage of reduction overall does not necessarily reflect the reduction in the relevant tissue, the body-wall muscle cells.

It will be of interest in future studies to examine whether the genes identified here for polyglutamine protein aggregation influence the folded state of other disease-associated aggregation-prone proteins (28–32). Given that our screen identified genes that have general and essential roles in cellular biosynthesis, we predict that the control of protein homeostasis will be important in development and aging, for example to suppress accumulated mutations and the age-dependent increase in the load of damaged proteins. The results that we present here offer an understanding of the etiology of protein misfolding diseases and experimental approach that may lead to the identification of novel gene targets for drug therapy of neurodegenerative diseases.

We thank members of the Plasterk and Morimoto laboratories for advice and comments on the manuscript. In particular, we thank Jim Morley, who provided the initial data that RNAi of HSF1 resulted in enhanced polyQ aggregation, and M. Amaral for advice. Support was provided from the Netherlands Organization for Scientific Research (NWO) (to E.A.A.N.), Fundação para a Ciência e a Tecnologia Ph.D. fellowship PRAXIS XXI BD/21451/99 (to S.M.G.), and a National Institutes of Aging Training Grant on Mechanisms in Aging and Dementia (to S.K.). R.H.A.P. was supported by a grant from the Research Institute of Diseases in the Elderly (RIDE), and R.I.M. was supported by the National Institutes of General Medical Sciences, the Huntington Disease Society of America Coalition for the Cure, and the Daniel F. and Ada L. Rice Foundation.

1. Taylor, J. P., Hardy, J. & Fischbeck, K. H. (2002) *Science* **296,** 1991–1995.
2. Soto, C. (2003) *Nat. Rev. Neurosci.* **4,** 49–60.
3. Driscoll, M. & Gerstbrein, B. (2003) *Nat. Rev. Genet.* **4,** 181–194.
4. Gusella, J. F. & MacDonald, M. E. (2000) *Nat. Rev. Neurosci.* **1,** 109–115.
5. Penney, J. B., Jr., Vonsattel, J. P., MacDonald, M. E., Gusella, J. F. & Myers, R. H. (1997) *Ann. Neurol.* **41,** 689–692.
6. Scherzinger, E., Sittler, A., Schweiger, K., Heiser, V., Lurz, R., Hasenbank, R., Bates, G. P., Lehrach, H. & Wanker, E. E. (1999) *Proc. Natl. Acad. Sci. USA* **96,** 4604–4609.
7. Scherzinger, E., Lurz, R., Turmaine, M., Mangiarini, L., Hollenbach, B., Hasenbank, R., Bates, G. P., Davies, S. W., Lehrach, H. & Wanker, E. E. (1997) *Cell* **90,** 549–558.
8. Satyal, S. H., Schmidt, E., Kitagawa, K., Sondheimer, N., Lindquist, S., Kramer, J. M. & Morimoto, R. I. (2000) *Proc. Natl. Acad. Sci. USA* **97,** 5750–5755.
9. Morley, J. F., Brignull, H. R., Weyers, J. J. & Morimoto, R. I. (2002) *Proc. Natl. Acad. Sci. USA* **99,** 10417–10422.
10. Hsu, A. L., Murphy, C. T. & Kenyon, C. (2003) *Science* **300,** 1142–1145.
11. Kim, S., Nollen, E. A., Kitagawa, K., Bindokas, V. P. & Morimoto, R. I. (2002) *Nat. Cell. Biol.* **4,** 826–831.
12. Cuppen, E., van Ham, M., Wansink, D. G., de Leeuw, A., Wieringa, B. & Hendriks, W. (2000) *Eur. J. Cell Biol.* **79,** 283–293.
13. Cummings, C. J., Mancini, M. A., Antalffy, B., DeFranco, D. B., Orr, H. T. & Zoghbi, H. Y. (1998) *Nat. Genet.* **19,** 148–154.
14. Kazemi-Esfarjani, P. & Benzer, S. (2000) *Science* **287,** 1837–1840.
15. Warrick, J. M., Chan, H. Y., Gray-Board, G. L., Chai, Y., Paulson, H. L. & Bonini, N. M. (1999) *Nat. Genet.* **23,** 425–428.
16. Fernandez-Funez, P., Nino-Rosales, M. L., de Gouyon, B., She, W. C., Luchak, J. M., Martinez, P., Turiegano, E., Benito, J., Capovilla, M., Skinner, P. J., *et al.* (2000) *Nature* **408,** 101–106.
17. DiFiglia, M., Sapp, E., Chase, K. O., Davies, S. W., Bates, G. P., Vonsattel, J. P. & Aronin, N. (1997) *Science* **277,** 1990–1993.
18. Kamath, R. S., Fraser, A. G., Dong, Y., Poulin, G., Durbin, R., Gotta, M., Kanapin, A., Le Bot, N., Moreno, S., Sohrmann, M., *et al.* (2003) *Nature* **421,** 231–237.
19. Dunn, A. Y., Melville, M. W. & Frydman, J. (2001) *J. Struct. Biol.* **135,** 176–184.
20. Garcia-Mata, R., Bebok, Z., Sorscher, E. J. & Sztul, E. S. (1999) *J. Cell Biol.* **146,** 1239–1254.
21. Siegers, K., Bolter, B., Schwarz, J. P., Bottcher, U. M., Guha, S. & Hartl, F. U. (2003) *EMBO J.* **22,** 5230–5240.
22. Feldman, D. E., Spiess, C., Howard, D. E. & Frydman, J. (2003) *Mol. Cell* **12,** 1213–1224.
23. Craig, E. A. (2003) *Curr. Biol.* **13,** R904–R905.
24. Willingham, S., Outeiro, T. F., DeVit, M. J., Lindquist, S. L. & Muchowski, P. J. (2003) *Science* **302,** 1769–1772.
25. Tavernarakis, N., Wang, S. L., Dorovkov, M., Ryazanov, A. & Driscoll, M. (2000) *Nat. Genet.* **24,** 180–183.
26. Timmons, L., Court, D. L. & Fire, A. (2001) *Gene* **263,** 103–112.
27. Morley, J. F. & Morimoto, R. I. (2003) *Mol. Biol. Cell.* **15,** 657–664.
28. Kraemer, B. C., Zhang, B., Leverenz, J. B., Thomas, J. H., Trojanowski, J. Q. & Schellenberg, G. D. (2003) *Proc. Natl. Acad. Sci. USA* **100,** 9980–9985.
29. Link, C. D. (1995) *Proc. Natl. Acad. Sci. USA* **92,** 9368–9372.
30. Oeda, T., Shimohama, S., Kitagawa, N., Kohno, R., Imura, T., Shibasaki, H. & Ishii, N. (2001) *Hum. Mol. Genet.* **10,** 2013–2023.
31. Spillantini, M. G., Crowther, R. A., Jakes, R., Hasegawa, M. & Goedert, M. (1998) *Proc. Natl. Acad. Sci. USA* **95,** 6469–6473.
32. Faber, P. W., Voisine, C., King, D. C., Bates, E. A. & Hart, A. C. (2002) *Proc. Natl. Acad. Sci. USA* **99,** 17131–17136.